Combined Streamline Upwind Petrov Galerkin Method and Segregated Finite Element Algorithm for Conjugate Heat Transfer Problems

Atipong Malatip, Niphon Wansophark, Pramote Dechaumphai*

Department of Mechanical Engineering, Faculty of Engineering, Chulalongkorn University, Patumwan, Bangkok, 10330, Thailand

A combined Streamline Upwind Petrov-Galerkin method (SUPG) and segregated finite element algorithm for solving conjugate heat transfer problems where heat conduction in a solid is coupled with heat convection in viscous fluid flow is presented. The Streamline Upwind Petrov-Galerkin method is used for the analysis of viscous thermal flow in the fluid region, while the analysis of heat conduction in solid region is performed by the Galerkin method. The method uses the three-node triangular element with equal-order interpolation functions for all the variables of the velocity components, the pressure and the temperature. The main advantage of the presented method is to consistently couple heat transfer along the fluid-solid interface. Four test cases, which are the conjugate Couette flow problem in parallel plate channel, the counter-flow in heat exchanger, the conjugate natural convection in a square cavity with a conducting wall, and the conjugate natural convection and conduction from heated cylinder in square cavity, are selected to evaluate efficiency of the presented method.

Key Words : Conjugate Heat Transfer, Finite Element Method

1. Introduction

Conjugate heat transfer problems are encountered in many practical applications, where heat conduction in a solid region is closely coupled with heat convection in an adjacent fluid. There are many engineering problems where conjugate heat transfer should be considered such as design of air-cooled packaging, heat transfer enhancement by the finned surfaces, design of thermal insulation, nuclear reactor design, design of solar equipment, heat transfer in a cavity with thermally conducting wall or internal baffle, etc. Most of the studies in this research area, however, employ the finite difference and the finite volume methods as the numerical tools. He et al.(1995) studied the conjugate problem using an iterative FDM/BEM method for parallel plate channel with constant outside temperature. Sugavanam et al.(1995) study a numerical investigation of conjugate heat transfer from a flush heat source on a conductive board in laminar channel flow. Chen and Han (2000) show the solution of a conjugate heat transfer problem using a finite difference SIMPLE-like algorithm. Schäfer and Teschauer (2001) used the finite volume method for analysis of both the fluid flow behavior and the solid heat transfer with thermal effect. Kang-Youl Bae et al.(2004) study on natural convection in a rectangular enclosure by using the finite volume method. The results from these problems show that both the finite difference and the finite volume methods can perform very well on the problems of interest, but some assumptions on heat transfer coefficients have to be made in order to compute the tem-

* Corresponding Author,
E-mail : fmepdc@eng.chula.ac.th
TEL : +66-2-218-6621; **FAX** : +66-2-218-6621
Department of Mechanical Engineering, Faculty of Engineering, Chulalongkorn University, Patumwan, Bangkok, 10330, Thailand. (Manuscript **Received** June 9, 2005; **Revised** July 3, 2006)

peratures along the fluid-solid interface. Furthermore, determination of the unknown temperatures and the heat fluxes at the fluid-solid interface is normally performed in an iterative way, usually through the use of the artificial heat transfer coefficient.

At present, a very few publications for solving the conjugate heat transfer problems by the finite element method have been proposed in the literature. Misra and Sarkar (1997) used the standard Galerkin formulation to solve the continuity, momentum and energy equations simultaneously.

In this paper, the streamline upwind Petrov-Galerkin method (Brooks and Hughes, 1982 ; Du Toit, 1998 ; Zienkiewicz and Taylor, 2000) is selected for the analysis of conjugate heat transfer problems. The method uses triangular elements with equal-order interpolation functions for the velocity components, the pressure and the temperature. A segregated solution algorithm (Rice and Schnipke, 1986 ; Wansophark and Dechaumphai, 2004 ; Kim and Sengupta, 2005) is also incorporated to solve the unknown variables separately for improving the computational efficiency. The main advantages of the presented scheme are illustrated and explained by using Figs. 1 and 2. Figure 1 shows typical control volumes of the fluid and solid cells along the fluid-solid interface used by the finite volume method. In the figure, the control volumes 1 and 2 are in the fluid region while the control volumes 3 and 4 are in the solid region. Because the heat conduction coefficients in solid and fluid regions are different, the harmonic mean of the heat conduction coefficient along the fluid-solid interface was introduced and assumed in the form (Patankar, 1980),

$$k_{interface}=\frac{2k_sk_f}{k_s+k_f} \tag{1}$$

where k_s and k_f are the heat conduction coefficients in the solid and the fluid region, respectively. The heat flux across the fluid-solid interface was then calculated using the assumed heat conduction coefficient. For the finite element method presented in the paper, the elements along the interface are shown in Fig. 2. The use of the finite element method, for both the fluid and solid

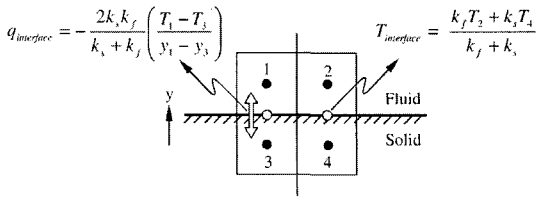

Fig. 1 Control volumes across fluid-solid interface used by the finite volume method

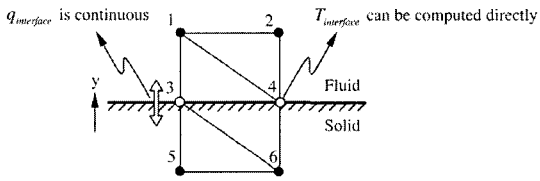

Fig. 2 Elements across fluid-solid interface in finite element method

regions with common nodes along the fluid- solid interface, provides convenience in analysis computation. At the same time, the use of the single finite element method in both the regions allows the fluid-solid interface temperatures to be computed directly without assuming the heat transfer coefficient. In addition, the continuity of the heat fluxes across the fluid and solid regions along the interface is also preserved automatically.

The paper starts from briefly describing the set of the partial differential equations that satisfy the law of conservation of mass, momentums and energy. Corresponding finite element equations are derived and the element matrices are presented. The computational procedure used in the development of the computer program is then described. Finally, the finite element formulation and the computer program are then verified by solving several examples that have exact solution and numerical solutions from other methods.

2. Theoretical Formulation and Solution Procedure

2.1 Governing equations

The governing equations for conjugate heat transfer problems consist of the conservation of mass which is called the continuity equation, the conservation of momentum in x and y-directions,

and the conservation of energy, as follows,

Continuity equation,

$$\frac{\partial u}{\partial x}+\frac{\partial v}{\partial y}=0 \tag{2a}$$

Momentum equations,

$$\rho\left[u\frac{\partial u}{\partial x}+v\frac{\partial u}{\partial y}\right]=-\frac{\partial p}{\partial x}+\mu\left[\frac{\partial^2 u}{\partial x^2}+\frac{\partial^2 u}{\partial y^2}\right] \tag{2b}$$

$$\rho\left[u\frac{\partial v}{\partial x}+v\frac{\partial v}{\partial y}\right]=-\frac{\partial p}{\partial y}+\mu\left[\frac{\partial^2 v}{\partial x^2}+\frac{\partial^2 v}{\partial y^2}\right]-\rho g(1-\beta(T-T_o)) \tag{2c}$$

Energy equation,

$$\rho c\left[u\frac{\partial T}{\partial x}+v\frac{\partial T}{\partial y}\right]=k\left[\frac{\partial^2 T}{\partial x^2}+\frac{\partial^2 T}{\partial y^2}\right]+\rho Q \tag{2d}$$

where u and v are the velocity components in the x and y-direction, respectively, ρ is the density, p is the pressure, μ is the viscosity, g is the gravitational acceleration constant, β is the volumetric coefficient of thermal expansion, T is the temperature, T_o is the reference temperature for which buoyant force in the y-direction vanishes, c is the specific heat, k is the coefficient of thermal conductivity and Q is the internal heat generation rate per unit volume. Equation (2d) can also be used for solving conduction heat transfer in solid by setting both the velocity components, u and v, as zero.

2.2 Finite element formulation

The three-node triangular element is used in this study. The element assumes linear interpolation functions for the velocity components, the pressure, and the temperature as,

$$u(x,y)=\sum N_i(x,y)\,u_i=\lfloor N\rfloor\{u\} \tag{3a}$$

$$v(x,y)=\sum N_i(x,y)\,v_i=\lfloor N\rfloor\{v\} \tag{3b}$$

$$p(x,y)=\sum N_i(x,y)\,p_i=\lfloor N\rfloor\{p\} \tag{3c}$$

$$T(x,y)=\sum N_i(x,y)\,T_i=\lfloor N\rfloor\{T\} \tag{3d}$$

where $i=1,2,3$; and N_i is the element interpolation functions.

The basic idea of the solution algorithm presented in this paper is to use the two momentum equations for solving both of the velocity components, use the continuity equation for solving the pressure, and use the energy equation for solving the temperature in solid and fluid regions. The finite element equations corresponding to the momentum, the continuity and the energy equations, are shown in next section.

2.2.1 Streamline upwind petrov-galerkin method

The basic idea of the streamline upwind method is to add diffusion, which acts only in the flow direction. Extended to a Petrov-Galerkin formulation, the standard Galerkin weighting functions are modified by adding a streamline upwind perturbation, p, for suppressing the non-physical spatial oscillation in the numerical solution, which again acts only in the flow direction. In this paper, the modified weighting function, W_i, can be expressed as, (Zienkiewicz and Taylor, 2000)

$$W_i=N_i+p=N_i+\frac{\alpha h}{2|U|}\left[u\frac{\partial N_i}{\partial x}+v\frac{\partial N_i}{\partial y}\right] \tag{4}$$

where α is calculated for each element from,

$$\alpha=\alpha_{opt}=coth\,Pe-\frac{1}{Pe} \tag{5a}$$

with

$$Pe=\frac{|U|h}{2\tilde{k}}\ \text{and}\ |U|=\sqrt{u^2+v^2} \tag{5b}$$

where Pe is the Peclet numbers, $|U|$ is mean resultant velocity and h is element size as shown in Fig. 3.

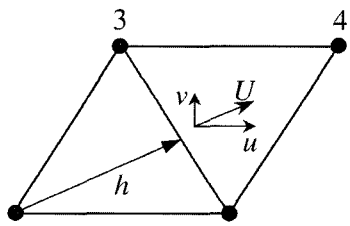

Fig. 3 The two-dimensional, element size h and streamline directions

2.2.2 Discretization of momentum equations

To derive the momentum equations that corresponded to the Streamline Upwind Petrov-Galerkin scheme, the Galerkin method of weighted residuals is employed by multiplying Eqs. (2b) and (2c) with the weighting function, N_i, except for the convection terms. The modified weighting function is applied to the convection terms in the equations, resulting in an inconsistent weighted residual formulation.

$$\int_\Omega W_i\rho\left(u\frac{\partial u}{\partial x}+v\frac{\partial u}{\partial y}\right)d\Omega = -\int_\Omega N_i\frac{\partial p}{\partial x}d\Omega+\int_\Omega N_i\mu\left(\frac{\partial^2 u}{\partial x^2}+\frac{\partial^2 u}{\partial y^2}\right)d\Omega \tag{6a}$$

$$\int_\Omega W_i\rho\left(u\frac{\partial v}{\partial x}+v\frac{\partial v}{\partial y}\right)d\Omega = -\int_\Omega N_i\frac{\partial p}{\partial y}d\Omega+\int_\Omega N_i\mu\left(\frac{\partial^2 v}{\partial x^2}+\frac{\partial^2 v}{\partial y^2}\right)d\Omega - \int_\Omega N_i\rho g[1-\beta(T-T_o)]d\Omega \tag{6b}$$

where Ω is integrated over the element domain.

Then the diffusion terms are integrated by parts using the Gauss theorem (Zienkiewicz and Taylor, 2000) to yield the element equations in the form,

$$[A]\{u\}=\{R_{px}\}+\{R_u\} \tag{7a}$$

$$[A]\{v\}=\{R_{py}\}+\{R_v\}+\{R_b\} \tag{7b}$$

where $[A]=[A_{conv}]+[A_{diff}]$.

The coefficient matrix $[A]$ contains the known contributions from the convection and diffusion terms. The element matrices and load vectors in Eqs. (7a) and (7b) are defined by,

$$[A_{conv}]=\rho\int_\Omega\{W\}\left(u\left[\frac{\partial N}{\partial x}\right]+v\left[\frac{\partial N}{\partial y}\right]\right)d\Omega \tag{8a}$$

$$[A_{diff}]=\mu\int_\Omega\left(\left\{\frac{\partial N}{\partial x}\right\}\left[\frac{\partial N}{\partial x}\right]+\left\{\frac{\partial N}{\partial y}\right\}\left[\frac{\partial N}{\partial y}\right]\right)d\Omega \tag{8b}$$

$$\{R_{px}\}=-\int_\Omega\{N\}\frac{\partial p}{\partial x}d\Omega \tag{8c}$$

$$\{R_{py}\}=-\int_\Omega\{N\}\frac{\partial p}{\partial y}d\Omega \tag{8d}$$

$$\{R_u\}=\mu\int_\Gamma\{N\}\left[\frac{\partial u}{\partial x}n_x+\frac{\partial u}{\partial y}n_y\right]d\Gamma \tag{8e}$$

$$\{R_v\}=\mu\int_\Gamma\{N\}\left[\frac{\partial v}{\partial x}n_x+\frac{\partial v}{\partial y}n_y\right]d\Gamma \tag{8f}$$

$$\{R_b\}=-\int_\Omega\{N\}[\rho g(1-\beta(T-T_o))]d\Omega \tag{8g}$$

where Γ is the element boundary. The element equations are assembled to yield the global equations for the velocity components. Such global equations are then modified for the specified velocity components along the boundaries prior to solving for the new velocity components.

2.2.3 Discretization of pressure equation

To derive the discretized pressure equation, the method of weighted residuals is applied to the continuity equation, Eq. (2a),

$$\int_\Omega N_i\left(\frac{\partial u}{\partial x}+\frac{\partial v}{\partial y}\right)d\Omega=-\int_\Omega\left(\frac{\partial N_i}{\partial x}u+\frac{\partial N_i}{\partial y}v\right)d\Omega + \int_\Gamma N_i(un_x+vn_y)d\Gamma=0 \tag{9}$$

where the integrations are performed over the element domain Ω and along the element boundary Γ; n_x and n_y are the direction cosines of the unit vector normal to element boundary with respect to x and y-direction, respectively. As mentioned earlier, the continuity equation is used for solving the pressure, but the pressure term does not appear in the continuity equation. For this reason, the relation between velocity components and pressure are thus required. Such relations can be derived from the momentum equations, Eqs. (6a) and (6b) as,

$$A_{ii}u_i=-\sum_{j\neq i}A_{ij}u_j+f_i^u-\int_\Omega N_i\frac{\partial p}{\partial x}d\Omega \tag{10a}$$

$$A_{ii}v_i=-\sum_{j\neq i}A_{ij}v_j+f_i^v-\int_\Omega N_i\frac{\partial p}{\partial y}d\Omega \tag{10b}$$

where f_i^u and f_i^v are the surface integral terms and the source term due to buoyancy. By assuming constant pressure gradient on an element, then,

$$u_i=\hat{u}_i-K_{pi}\frac{\partial p}{\partial x} \tag{11a}$$

$$v_i=\hat{v}_i-K_{pi}\frac{\partial p}{\partial y} \tag{11b}$$

where

$$\hat{u}_i=\frac{-\sum_{j\neq 1}A_{ij}u_j+f_i^u}{A_{ii}} \tag{12a}$$

$$\hat{v}_i=\frac{-\sum_{j\neq 1}A_{ij}v_j+f_i^v}{A_{ii}} \tag{12b}$$

$$K_{pi}=\frac{\int_\Omega N_i d\Omega}{A_{ii}} \tag{12c}$$

By applying the element velocity interpolation functions, Eqs. (3a) and (3b), into the continuity equation, Eq. (9),

$$-\int_\Omega \frac{\partial N_i}{\partial x}(N_j u_j)\,d\Omega-\int_\Omega \frac{\partial N_i}{\partial y}(N_j v_j)\,d\Omega +\int_\Gamma N_i(un_x+vn_y)\,d\Gamma=0 \tag{13}$$

nd introducing the nodal velocities u_j and v_j from Eqs. (10a) and (10b), then Eq. (13) becomes,

$$\int_\Omega \frac{\partial N_i}{\partial x}(N_jK_{pj})\frac{\partial p}{\partial x}d\Omega+\int_\Omega \frac{\partial N_i}{\partial y}(N_iK_{pj})\frac{\partial p}{\partial y}d\Omega =\int_\Omega \frac{\partial N_i}{\partial x}(N_j\hat{u}_j)\,d\Omega+\int_\Omega \frac{\partial N_i}{\partial y}(N_j\hat{v}_j)\,d\Omega -\int_\Gamma N_i(un_x+vn_y)\,d\gamma \tag{14}$$

Finally, applying the element pressure interpolation functions, Eq. (3c), the above element equations can be written in matrix form with unknowns of the nodal pressures as,

$$[K_x+K_y]\{p\}=\{F_u\}+\{F_v\}+\{F_b\} \tag{15}$$

where

$$[K_x]=\int_\Omega\left\{\frac{\partial N}{\partial x}\right\}(N_jK_{pj})\left\lfloor\frac{dN}{dx}\right\rfloor d\Omega \tag{16a}$$

$$[K_y]=\int_\Omega\left\{\frac{\partial N}{\partial y}\right\}(N_jK_{pj})\left\lfloor\frac{dN}{dy}\right\rfloor d\Omega \tag{16b}$$

$$\{F_u\}=\int_\Omega(N_j\hat{u}_j)\left\{\frac{\partial N}{\partial x}\right\}d\Omega \tag{16c}$$

$$\{F_v\}=\int_\Omega(N_j\hat{v}_j)\left\{\frac{\partial N}{\partial y}\right\}d\Omega \tag{16d}$$

$$\{F_b\}=-\int_\Gamma\{N\}(un_x+vn_y)\,d\Gamma \tag{16e}$$

The above element pressure equations are assembled to form the global equations, boundary conditions for the specified nodal pressures are imposed prior to solving for the updated nodal pressures.

2.2.4 Discretization of energy equation

The finite element equations corresponding to the energy equation are derived using an approach which is similar to the momentum equations. The modified weighting function is applied to the convection term in the energy equation, Eq. (2d). The standard Galerkin method is then applied to yield the element equations and the integrated over the element domain Ω,

$$\int_\Omega W_i\rho c\left(u\frac{\partial T}{\partial x}+v\frac{\partial T}{\partial y}\right)d\Omega =\int_\Omega N_ik\left(\frac{\partial^2 T}{\partial x^2}+\frac{\partial^2 T}{\partial y^2}\right)d\Omega+\int_\Omega N_i\rho Q d\Omega \tag{17}$$

and then the diffusion terms are integration by parts using the Gauss theorem to yield the element equations in the form,

$$[A^T]\{T\}=\{R\}+\{Q\} \tag{18}$$

where $[A^T]=[A^T_{conv}]+[A^t_{diff}]$.

The matrix $[A^T]$ consists of the contributions from the convection and diffusion terms. The element matrices and load vectors $\{R\}$ and $\{Q\}$ represent the heat flux along the element boundary and internal heat generation, respectively as,

$$[A^T_{conv}]=\rho c\int_\Omega\{W\}\left(u\left\lfloor\frac{\partial N}{\partial x}\right\rfloor+v\left\lfloor\frac{\partial N}{\partial y}\right\rfloor\right)d\Omega \tag{19a}$$

$$[A^T_{diff}]=k\int_\Omega\left(\left\{\frac{\partial N}{\partial x}\right\}\left[\frac{\partial N}{\partial x}\right]+\left\{\frac{\partial N}{\partial y}\right\}\left[\frac{\partial N}{\partial y}\right]\right)d\Omega \tag{19b}$$

$$\{R\}=k\int_\Gamma\{N\}\left(\frac{\partial T}{\partial x}n_x+\frac{\partial T}{\partial y}n_y\right)d\Gamma \tag{19c}$$

$$\{Q\}=\rho\int_\Omega\{N\}Q d\Omega \tag{19d}$$

These element equations are again assembled to yield the global temperature equations. Appropriate boundary conditions are applied prior to solving for the new temperature values.

2.2.5 Computational procedure

The computational procedure is described in this section. A set of initial nodal velocity components, pressures, and temperatures are first assumed. The new nodal temperatures are computed using Eq. (18). The new nodal velocity components and pressures are then computed using Eqs. (7a) and (7b) and Eq. (15), respectively. The nodal velocity components are then updated using Eqs. (10a) and (10b) with the computed nodal pressures. This process is continued until the specified convergence criterion is met. Such segregated solution procedure helps reducing the computer storage because the equations for the velocity components, the pressure, and the temperature are solved separately.

3. Results

In this section, four example problems are presented. The first example, conjugate Couette flow problem in parallel plate channel, is chosen to evaluate the finite element formulation and to validate the developed computer program. The second, the third and the fourth examples, counter-flow in heat exchanger, conjugate natural convection in a square cavity with a conducting wall and conjugate natural convection and conduction from heated cylinder in square cavity, respectively, are used to illustrate the efficiency of the presented scheme for the analysis of conjugate heat transfer problems.

3.1 Conjugate couette flow problem in parallel plate channel

The first example for evaluating the finite element formulations and validating the developed computer programs is the problem of conjugate Couette flow problem in parallel plate channel (White, 1991). The problem statement is shown in Fig. 4 with a fluid between the upper wall that moves at a constant velocity and a stationary conducting solid. The other side of the conducting solid is maintained at a constant temperature that is higher than the constant temperature of the opposing channel wall. The computed solutions are compared with the analytical solutions

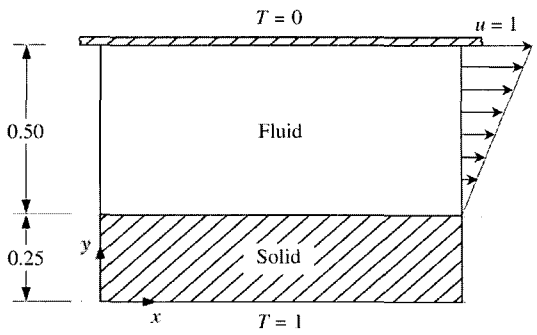

Fig. 4 Conjugate couette flow problem in parallel plate channel

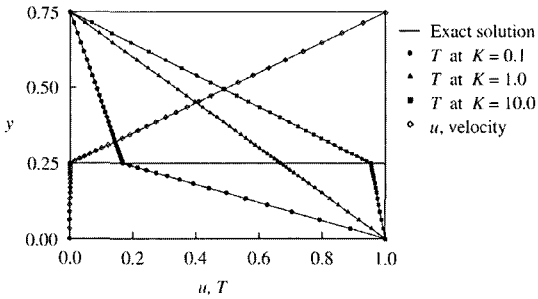

Fig. 5 Comparison of conjugate benchmark solution for couette flow conditions

(White, 1991) as shown in Fig. 5. The figure show that the solutions obtained from the presented finite element scheme shows excellent agreement with the analytical solutions for varying conductivity ratios, $K=k_s/k_f$. The numerical results of the temperatures from the Streamline Upwind Petrov-Galerkin method are compared within 0.04% while the velocities compared within 0.01% of the analytical solutions.

3.2 Conjugate counter flow heat exchanger

To further validate the numerical scheme, a conjugate counter flow heat exchanger problem is selected as the second test case. This heat exchanger consists of two parallel flow passages with widths a_1 and a_3, separated by a solid plate with thickness of a_2 as shown in Fig. 6. The outer walls of the flow passages are assumed to be adiabatic. The same properties and uniform inlet velocity and temperature profiles are assumed for the hot and cold fluids. The parameters adopted in the computation are as follows, geometrical

sizes $a_1=a_2=a_3=0.1$ and $L=1.0$, the flow parameters in upper channel $u_1=0.2$, $T_1=800$, $Re=133.33$ and $Pr=0.75$, the flow parameters in lower channel $u_2=0.1$, $T_2=300$, $Re=66.67$ and $Pr=0.75$, conduction ratio $K=5$. The finite element model, consisting of 1,763 nodes and 3,360 triangles as shown in Fig. 7, is used in this study. Fig. 8 shows the predicted temperature contours in entire domain. The predicted temperature distributions at $x=L/2$ from presented scheme is compared with the finite volume results from Chen and Han (2000) as shown in Fig. 9. The figure also shows good agreement of the solutions.

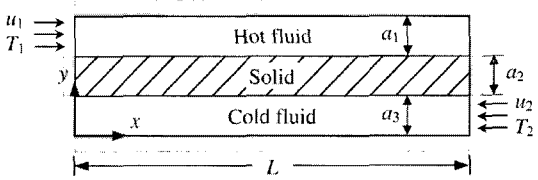

Fig. 6 A conjugate counter flow heat exchanger

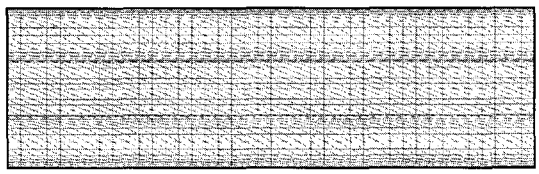

Fig. 7 Finite element model for conjugate counter flow heat exchanger

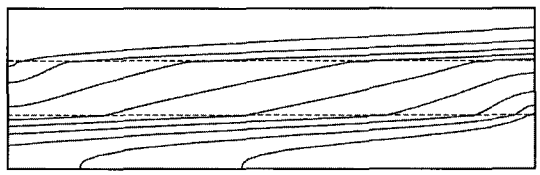

Fig. 8 Predicted temperature contours for a conjugate counter flow heat exchanger

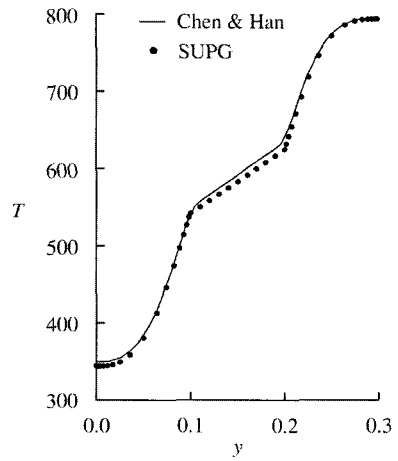

Fig. 9 The temperature profiles at $x=L/2$ for a conjugate counter flow heat exchanger

3.3 Conjugate natural convection in a square cavity with a conducting wall

To further evaluate the efficiency of the presented schemes, the problem of conjugate natural convection in a square cavity with a conducting wall as shown in Fig. 10, is selected. The fluid in the cavity is heated from the higher temperature solid wall along the left side and maintained at zero temperature along the right side, all other boundaries are insulated. The finite element model

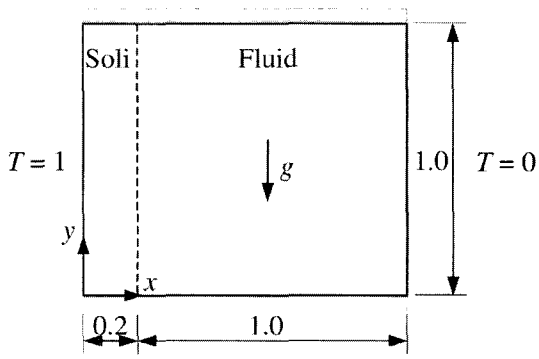

Fig. 10 Conjugate natural convection problem

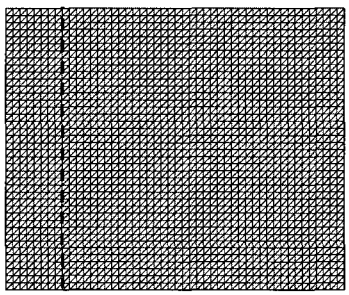

Fig. 11 Finite element model for the conjugate natural convection problem

for both the solid wall and fluid region consisting of 2,009 nodes and 3,840 triangles is shown in Fig. 11. Figs. 12 and 13 show the predicted streamline and temperature contours for the different thermal conductivity ratios of $K=1$ and 10 at the Grashof numbers of 10^3 and 10^5, respectively. The temperature and the heat flux distributions along the solid-fluid interface with the variation of conduction ratio, K, are shown in Figs. 14(a) and (b), respectively. In addition, Table 1 compares the predicted average Nusselt numbers along the interface, $\overline{Nu}_{x=0.2}$, with the results using the

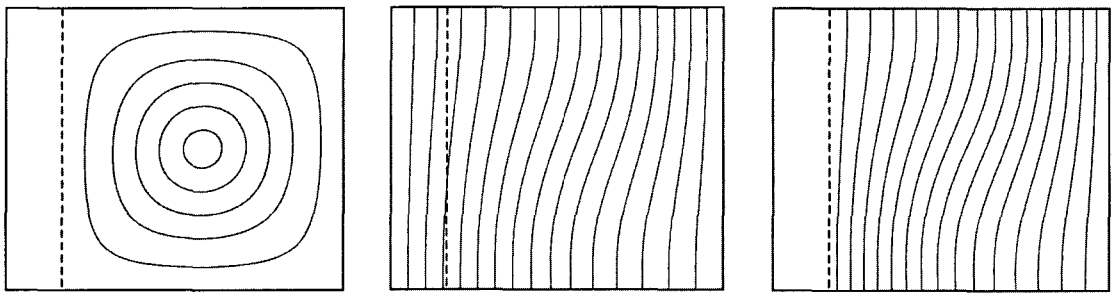

Fig. 12 (a) Streamline contours for $K=10$, (b) Temperature contours for $K=1$ and (c) Temperature contours for $K=10$, all at $Gr=10^3$

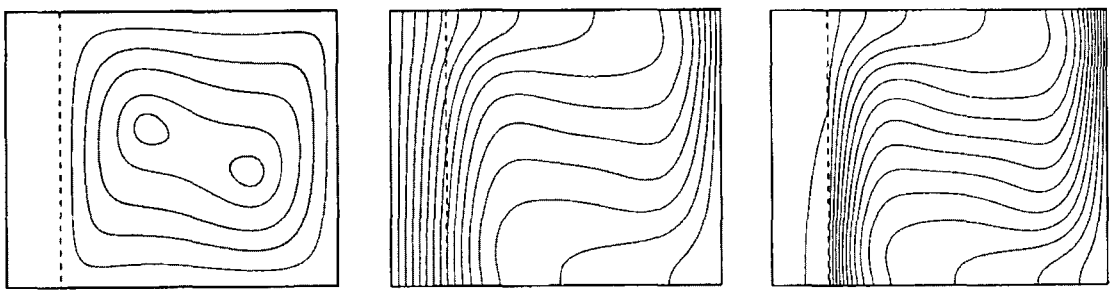

Fig. 13 (a) Streamline contours for $K=10$, (b) Temperature contours for $K=1$ and (c) Temperature contours for $K=10$, all at $Gr=10^5$

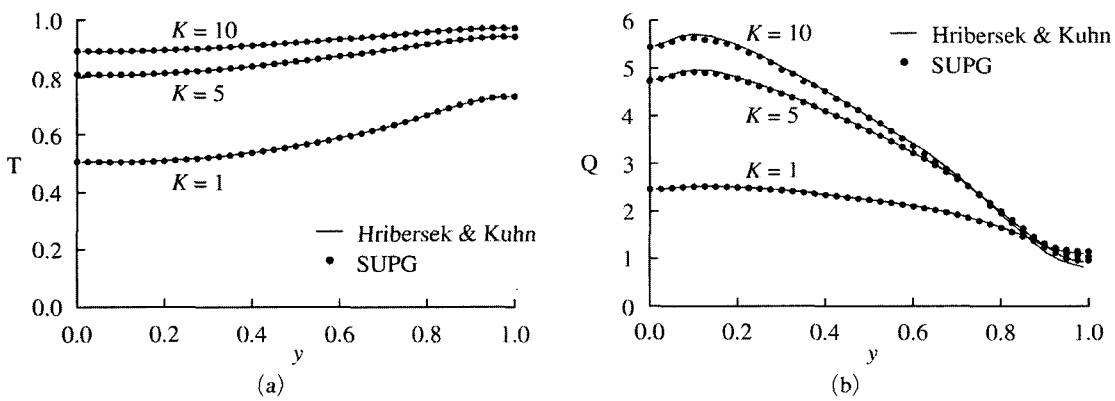

Fig. 14 (a) Interface temperatures and (b) Interface heat fluxes, all at $Gr=10^5$

Table 1 Variation of the overall nusselt numbers

Gr	Average nusselt number along interface (% difference from Ref.(Zienkiewicz and Taylor, 2000))			
Conductivity ratio, $K=k_s/k_f$		1	5	10
10^3	Hribersek (Zienkiewicz and Taylor, 2000)	0.87	1.02	1.04
10^3	SUPG	0.87 (0.0%)	1.02 (0.0%)	1.04 (0.0%)
10^5	Hribersek (Zienkiewicz and Taylor, 2000)	2.08	3.42	3.72
10^5	SUPG	2.07 (0.48%)	3.39 (0.87%)	3.67 (1.34%)

boundary-domain integral method by Hribersek (2000). The table shows good agreement of the average Nusselt numbers for both the temperature and the heat flux.

3.4 Conjugate natural convection and conduction from heated cylinder in square cavity

The last example of a high temperature cylinder enclosed by a square cavity as shown in Fig. 15, is selected to demonstrate the use of the presented method for the problem with a more complex geometry. Both the vertical side walls of the square cavity are isothermal. The upper horizontal boundary is surrounded by a solid material. The upper boundary of this solid region is considered as adiabatic. The lower horizontal boundary of the fluid cavity is also an adiabatic boundary. Due to the symmetry of flow solution, only the right half of the enclosure was analyzed. The finite element model consisting of 1,821 nodes and 3,450 triangles, as shown in Fig. 16, is used in this study. Figure 17 shows the predicted streamline and temperature contours vary with the thermal conductivity ratios and the Rayleigh numbers. Figure 18 shows the predicted temperature distributions of lower adiabatic boundary at $y=0$, interface of fluid-solid regions at $y=1$, and the upper adiabatic boundary at $y=1.2$. This picture represents the different thermal conductivity ratios of $K=0.1$, 1, 5 and 10, respectively, at the Rayleigh number of 10^4 and is compared with the results from Dong and Li (2004). The figure shows good agreement of the solutions obtained from the presented scheme.

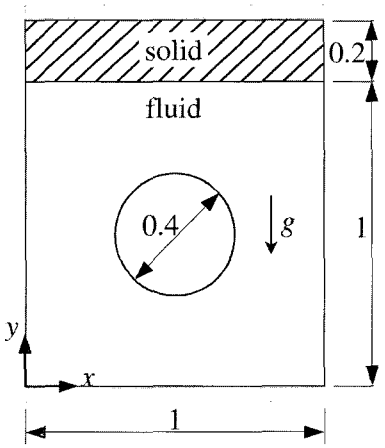

Fig. 15 Conjugate natural convection from heated cylinder in square cavity problme

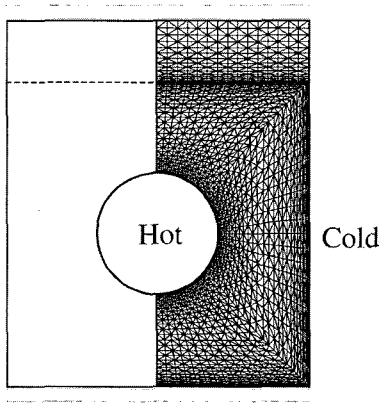

Fig. 16 Finite element model for heated cylinder in square cavity problem

In addition, the average Nusselt number, $\overline{Nu}$, was also investigated in this research, the average Nusselt number can be calculated by,

$$Nu_{mean}=\frac{1}{2\pi r}\oint Nu\, ds \tag{20}$$

which

$$Nu=\left|\frac{\partial T}{\partial x}\right|\times\frac{|x-x_c|}{r}+\left|\frac{\partial T}{\partial y}\right|\times\frac{|y-y_c|}{r} \tag{21}$$

where x_c, y_c are the center coordinates of the high temperature cylinder and r is radius of cylinder.

Table 2 gives a comparison of $\overline{Nu}$ at the cylinder's surface with results of Dong and Li. From the table, it can be concluded that the overall mean Nusselt number increases with the increase

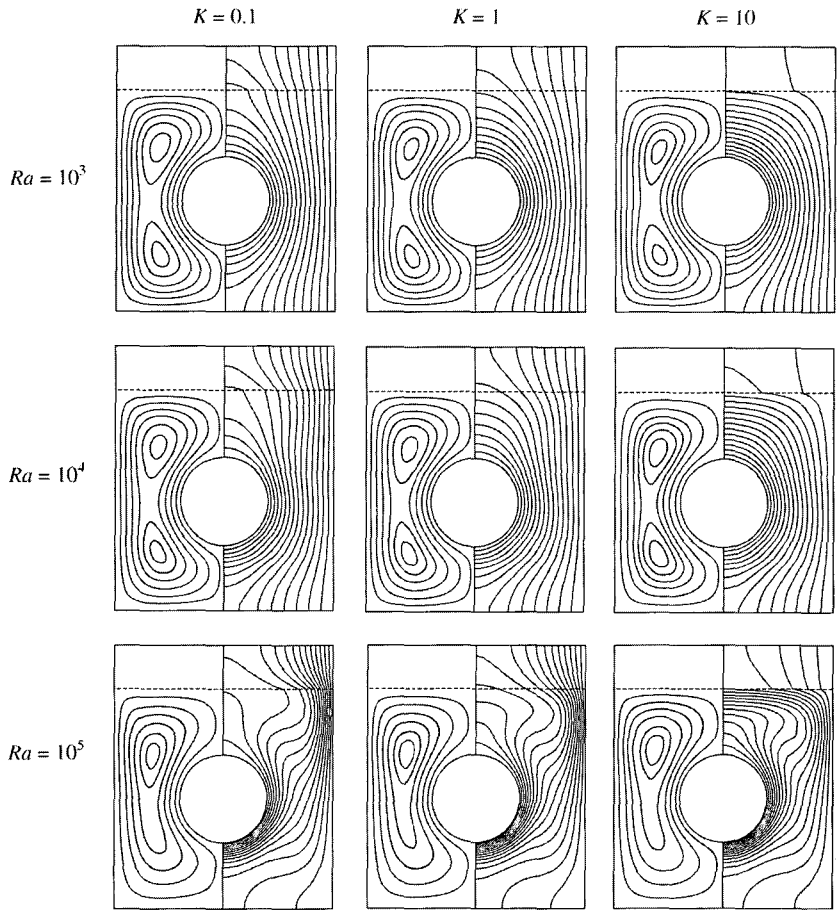

Fig. 17 Streamline and temperature contours for K=0.1, 1 and 10, at $Ra=10^3$, 10^4, and 10^5

Table 2 Variation of the overall mean Nusselt numbers along cylinder (% difference from Ref.(Patankar, 1980))

Ra		Conductivity ratio, $K=k_s/k_f$			
		0.1	1	5	10
10^3	SUPG	3.78	3.95	4.19	4.28
10^4	Dong and Li, 2004 (Patankar, 1980)	4.05	4.20	—	4.49
10^4	SUPG	3.99 (1.48%)	4.13 (1.67%)	4.35	4.43 (1.34%)
10^5	SUPG	6.84	6.97	7.23	7.35
10^6	SUPG	12.10	12.26	12.70	13.00

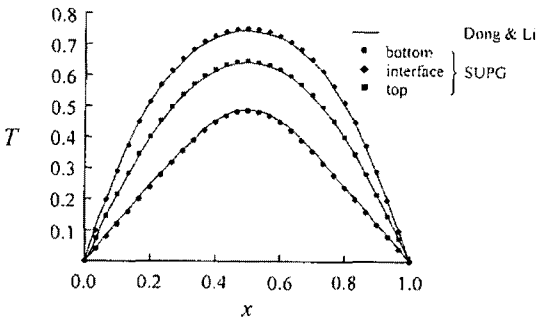

(a) $K=0.1$

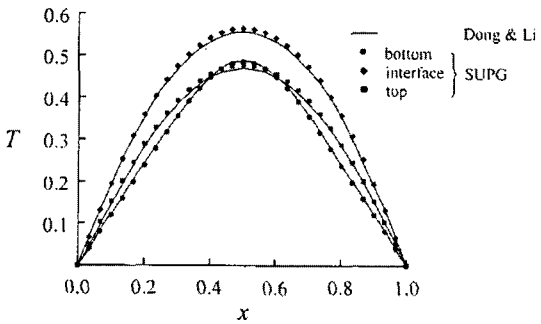

(b) $K=1.0$

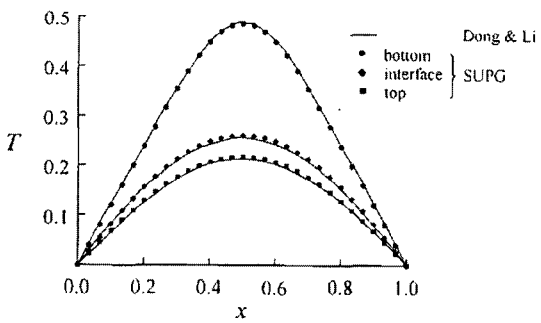

(c) $K=5.0$

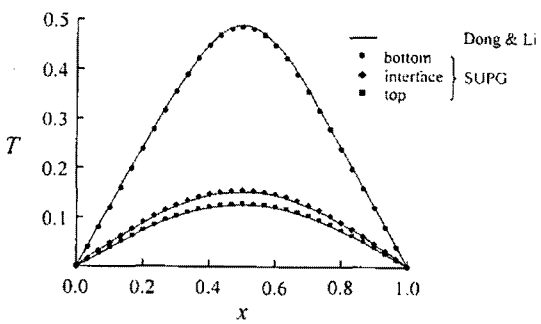

(d) $K=10.0$

Fig. 18 Compared the temperature distributions for conjugate natural convection and conduction from heated cylinder in square caviuty for $K=0.1$, 1, 5 and 10, all at $Ra=10^4$

of thermal conductivity ratios and the Rayleigh numbers. The table shows good agreement of the solutions obtained from the two methods.

4. Conclusions

A coupled finite element method for conjugate heat transfer problems was presented. The method combines the viscous thermal flow analysis of the fluid region and the heat transfer analysis in the solid region together. The finite element formulation and its computational procedure were first described. The flow analysis used a segregated solution algorithm to compute the velocities, the pressure and the temperature separately for improving the computational efficiency. The convection terms in the momentum and the energy equations are treated by the Streamline Upwind Petrov-Galerkin method to suppress the non-physical spatial oscillation in the numerical solutions. All the finite element equations were derived and a corresponding computer program was developed. The efficiency of the coupled finite element method has been evaluated by several examples that were previously performed using other methods. These examples highlight the benefit of the combined finite element method that can simultaneously model and solve both the fluid and solid regions, as well as to compute the temperatures along the fluid-solid interface directly.

Acknowledgements

The authors are pleased to acknowledge the Thailand Research Fund (TRF) for supporting this research work.

References

Bae, K. Y., Jeong, H. M. and Chung, H. S., 2004, "Study on Natural Convection in a Rectangular Enclosure with a Heating Source," *KSME International Journal*, Vol. 18, pp. 294~301.

Brooks, A. N. and Hughes, T. J. R., 1982, "Streamline Upwind/Petrov-Galerkin Formulations for Convection Dominated Flows with Particular Emphasis on the Incompressible Navier-

Stokes Equations," *Computer Methods in Applied Mechanics and Engineering*, Vol. 32, pp. 199~259.

Chen, X. and Han, P., 2000, "A Note on The Solution of Conjugate Heat Transfer Problems Using SIMPLE-Like Algorithms," *International Journal of Heat and Fluid Flow*, Vol. 21, pp. 463~467.

Dong, S. F. and Li, Y. T., 2004, "Conjugate of Natural Convection and Conduction in a Complicated Enclosure," *International Journal of Heat and Mass Transfer*, Vol. 47, pp. 2233~2239.

Du Toit, C. G., 1998, "Finite Element Solution of Navier-Stokes Equations for Incompressible Flow using a Segregated Algorithm," *Computer Methods in Applied Mechanics and Engineering*, pp. 131~141.

He, M., Kassab, A. J. Bishop, P. J. and Minardi, A., 1995, "An Iterative FDM/BEM Method for the Conjugate Heat Transfer Problem — Parallel Plate Channel with Constant Outside Temperature," *Engineering Analysis with Boundary Elements*, Vol. 15, pp. 43~50.

Hribersek, M. and Kuhn, G., 2000, "Conjugate Heat Transfer by Boundary-Domain Integral Method," *Engineering Analysis with Boundary Elements*, Vol. 24, pp. 297~305.

Kim, M. S. and Sengupta, A., 2005, "Unsteady Viscous Flow over Elliptic Cylinders At Various Thickness with Different Reynolds Numbers," *Journal of Mechanical Science and Technology (KSME I. J.)*. Vol. 19, pp. 877~886.

Misra. D. and Sarkar. A., 1997. "Finite Element Analysis of Conjugate Natural Convection in a Square Enclosure with a Conducting Vertical Wall," *Computer Methods in Applied Mechanics and Engineering*, Vol. 141, pp. 205~219.

Patankar, S. V., 1980, *Numerical Heat Transfer and Fluid Flow*, McGraw-Hill, New York.

Rice, J. G. and Schnipke, R. J., 1986, "An Equal-Order Velocity-Pressure Formulation that does not Exhibit Spurious Pressure Modes," *Computer Methods in Applied Mechanics and Engineering*, Vol. 58, pp. 135~149.

Schäfer, M. and Teschauer, I., 2001, "Numerical Simulation of Coupled Fluid-Solid Problems," *Computer Methods in Applied Mechanics and Engineering*, Vol. 190, pp. 3645~3667.

Sugavanam, R., Ortega, A. and Choi, C. Y., 1995, "A Numerical Investigation of Conjugate Heat Transfer from a Flush Heat Source on a Conductive Board in Laminar Channel Flow," *International Journal of Heat and Mass Transfer*, Vol. 38, pp. 2969~2984.

Wansophark, N. and Dechaumphai, P., 2004, "Combined Adaptive Meshing Technique and Segregated Finite Element Algorithm for Analysis of Free and Forced Convection Heat Transfer," *Finite Elements in Analysis and Design*, Vol. 40, pp. 645~663.

White, F. M., 1991, *Viscous Fluid Flow*, 2nd ed McGraw-Hill, New York.

Zienkiewicz, O. C. and Taylor, R. L., 2000, *The Finite Element Method*, 5th ed (McGraw-Hill Butterworth-Heinemann, Oxford, 2000).